ANALYSIS OF WEB SPREADING INDUCED BY THE CONCAVE ROLLER

by

R. D. Delahoussaye and J. K. Good

Oklahoma State University
Stillwater, Oklahoma

ABSTRACT

This paper describes the development of a model for predicting the elastic deformations and stresses in a web crossing a concave (or negative crown) roller. The Finite Element Method was used to compute web displacements, forces and stresses. A preprocessor was developed to automatically convert the web material properties and roller geometry into a FEM mesh and a set of boundary conditions. The boundary conditions which produce web spreading were developed and incorporated into the model. The principal boundary conditions in this model are derived from the assumption that there is sufficient friction between the web and the roller to prevent slipping. Because of the nonlinear nature of the traction between the web and the roller, an iterative Finite Element solution technique was used. The model was used to perform a study of the effects of variations in geometry, material properties and operating conditions on the spreading behavior of the web/roller system. The results of this study are presented.

INTRODUCTION

A web is defined as any material in continuous flexible strip form [1]. The flexibility of the web is derived from the fact that the material thickness is small compared to the length and width of the material.

Web materials are usually delivered in the form of rolls, because of their compactness and ease of handling. Most web handling systems include equipment to unwind the roll of web material, transport it through the various manufacturing processes, and rewind it onto a roll. The material is usually supported, guided, and propelled by rollers.

The commercial pressures for increased productivity require higher and higher line speeds. As the speed of the line increases, the static and dynamic forces acting on the web become more extreme, increasing the likelihood of defects in the material. Wrinkling is one of the most common web defects.

Several devices have been developed to remove wrinkles from webs or prevent them from forming. The most common spreading devices are the D-Bar spreader, the curved axis (Mt. Hope) roller, and the concave roller. The concave roller is the subject of this paper. The curved axis roller is described in a companion paper.

The construction of the concave roller is very much like the cylindrical rollers used in most web handling equipment. The major difference is that the roller is not cylindrical, but instead has a smaller diameter at the center, and a larger diameter at the ends. The concave roller is closely related to the crowned roller which has been used for many years as a means of keeping power transmission belts centered on their pulleys.

The concave roller is much more dependent on surface traction between the web and the roller than is the curved axis roller. Without sufficient friction, the concave roller can actually increase the likelihood of wrinkles. This is the primary disadvantage of the concave roller. The primary advantage of the concave roller over the curved axis roller is its similarity to the cylindrical roller. The concave roller can be made of the same materials, and have the same bearing configuration as the other rollers on the machine. This means that the concave roller can be designed to survive in the same environment as other rollers on the machine.

BACKGROUND

Swift [2] developed a design model for the crowned roller based on treating the belt as a beam bending due to an applied couple. Sassaki, Hira, Abe, Yangagishima, Shimoyama, and Tahara [3] performed both analytical and experimental investigations on the effect of crowned rollers used in the annealing furnace of a steel mill.

Shelton [4] used the idea of the idle arc as described by Swift to develop the principle of web transport. This principle is applied in much of the work in web guidance and control, and is used in developing the boundary conditions for the curved axis models. Shelton and Reid [5],[6] developed models for the lateral dynamics of webs and applied these models to web guide control systems. These web guide control systems generally rely on lateral shifting and pivoting of intermediate rollers to steer the web. The most important principle governing these devices is that the web will seek to align itself perpendicular to a roller in the entry span to that roller. Shelton used the equation for beam bending to model the lateral motion of the web due to the moments induced by the steering rollers. Shelton [7] also used the principles of web transport to investigate the dynamics of web tension control.

Pfeiffer [8] used the web transport principle and simple concepts from both narrow and wide web systems to offer rules of thumb for web guidance. He describes the spreading mechanism of the curved axis roller and the D-bar spreader. He also discusses factors governing the traction between the web and the roller.

Butler [9] describes a novel application of the concave roller. Concave rollers are being used to remove a condition called "bow" from fabric. Bow occurs in fabric when the fibers of the material are shifted in the machine direction, and no longer align properly in the cross machine direction.

Daly [10] investigated the factors controlling traction between webs and their carrying rolls. Proper traction is a critical factor in the performance of both the concave roller and the curved axis roller.

Leport [11] developed a three-dimensional FEM model of the concave roller, and Kliewer [12] continued working with Leport's model, searching for a reasonable set of geometric boundary conditions. They both used the method given in Zienkiewicz's text [13] on Finite Element methods which illustrates using a collection of planar elements to model three dimensional shells.

CONCAVE ROLLER MODEL SURFACE GEOMETRY

The total surface geometry model of the concave rollers requires the following information:

(1) The nominal dimensions of all the parts of the model. This includes the length and width of the web, the shape and orientation of the roller, and the angle of wrap between the web and the roller.
(2) The unstrained coordinates of the discretized shape. These are the locations of the nodes used to define the elements.
(3) The directions of a coordinate system normal to the nominal deformed surface at each node location.
(4) The known nodal deformations described in the node normal coordinate system. This includes all deformations normal to the surface, as well as any known deformations in the plane of the web surface.

This geometry information is calculated independently for the three major sections of the roller models: the entry span, the web contacting the roller, and the exit span.

Figure 1 is a schematic showing the nominal geometry of a web over a concave roller. The dimensions indicated in the figure are the basis for calculating the nodal locations, directions, and deformations required by the concave roller model. The geometry of the concave roller system has an axis of symmetry parallel to the direction of motion of the web (the machine direction). The roller model takes advantage of this symmetry by storing information for only one half of the total geometry.

In addition to the machine direction line of symmetry, the concave roller system has a line of symmetry in the cross machine direction. It is located on the roller at one half of the indicated wrap angle. Although this is a geometric line of symmetry, the boundary conditions to be described later are not symmetric about this line. For this reason, this symmetry is not used in the model.

Because the roller geometry is not a simple cylinder, the web material cannot conform itself to the surface of the roller without being strained. In order to properly calculate the strains and stresses imposed on the web when conforming to the roller shape, the web FEM mesh is first assembled as if it were wrapped around a cylindrical roller. This roller has a diameter equal to the average diameter of the concave roller. This is shown in figure 2.

From this unstrained position, the web is then deformed to conform to the roller as shown in the figure. Because the diameter of the roller varies in the cross machine direction, the magnitude of the deformation also varies. The figure shows the deformation at the outer edge of the web. For the simple geometry of the concave roller, all of the deformation required to conform the web to the roller are in the direction normal to the surface of the roller. This is modeled in the program as the local Z coordinate. Because all of the Z coordinate deformations are known in advance, those degrees of freedom are not stored explicitly in the FEM stiffness matrix. Instead, the effect of those deformations are assembled into the system force vector.

For each node location in the model, the directions of a coordinate system normal to the surface must be calculated. For the concave roller, these directions can be calculated as the concatenation of two simple rotations. The first is a rotation about the global X axis to align the coordinate system with the curvature of the roller at a point on top of the roller. The second is a rotation of this new coordinate system about the global Y axis to align the system with the wrap angle at the node location.

THE BOUNDARY CONDITIONS FOR THE MODELS

The most critical factor in correctly predicting deformations and stresses in the spreading rollers is the application of the proper boundary conditions. The boundary conditions used in the models are:

(1) Zero Y-direction (cross machine direction) displacements at all nodes on the centerline of the web. Because of the axis of symmetry in both of the rollers at the centerline of the web, only one half of the web is modeled. The web centerline is therefore one of the boundaries of the remaining portion of the web that is modeled.

(2) Fixed X-direction (machine direction) displacements at the beginning of the entry span and the end of the exit span. These displacements are calculated from the simple 1-D tension model using the dimensions of the web and the nominal line tension.

(3) Fixed X-direction displacements at all nodes in contact with the roller. The first row on nodes on the roller is the zero displacement reference point for displacements due to line tension. Additional X-directions displacements are added to the displacements due to line tension.

(4) Multi-point constraints in the Y-direction for all nodes in contact with the roller.

The multi-point constraints are used to implement the three physical boundary conditions which cause the spreading deformations. First, the state of strain in the free span immediately upstream from the roller contact point is identical to the state of strain on the roller immediately after the contact point. The second is: given sufficient friction, the web material will remain in contact with the surface of the roller. This is the No Slip boundary condition. Finally, given sufficient friction, the web material will be oriented normal to the roller at the initial point of contact with the roller. This is the Normal Entry boundary condition.

The governing effect in the behavior of the concave roller is the velocity of points on the surface of the roller in contact with the web. The velocity magnitude varies across the width of the roller. The velocity direction is uniform and is aligned parallel to the machine direction. This is caused by a uniform roller angular velocity combined with a non-uniform roller diameter and is shown in figure 3.

Because the roller velocity at the edge of the web is faster than the velocity at the center, the concave roller tries to shear the material at the edge of the web ahead of the material at the center. This is a local effect which causes a higher machine direction stress at the edge of the web that at the centerline of the web immediately before the web contacts the roller. These shearing displacements are shown in figure 4.

These shearing displacements are calculated from a simple FEM model of the entry span using the following procedure.

(1) The strain profile of the material on the web due to the roller diameter profile is calculated. This is a differential strain profile. The strain at the location on the roller which has the same diameter as the average roller diameter is defined to be zero.
(2) Using this differential strain profile and a simple 1-D tension model, the differential force at each node required to maintain this strain profile is calculated.
(3) A 2-D FEM model of the entry span is assembled.
(4) The nodes at the beginning of the entry span are frozen to zero machine direction displacements.
(5) The differential force profile is applied to the other end of the entry span.
(6) This FEM analysis yields a set of differential displacements. These displacements are the shearing displacements that are applied as boundary conditions to the full model of the roller.

There is another effect which induces a machine direction strain profile on the nodes of the roller. For constant mass flow in the machine direction, the material in contact with the roller at the edge of the web must have a higher MD strain than the material at the center of the roller. This compensates for the higher velocity at the edge of the web. Because of the way the unstrained web is assembled, this effect is induced without additional machine direction displacements. This is illustrated in figure 5.

The final boundary conditions required for the concave roller enforce the no slip condition over the roller. Given sufficient friction, a point on the web should travel at precisely the same velocity (magnitude and direction) as the point it is contacting on the roller. The previous boundary conditions assured that the velocity magnitude is matched. Additional constraints are required to match the velocity direction. Because the concave roller is axisymmetric about a line through its center of rotation, all points on the surface of the roller move in a circle. These circles are all in planes that are perpendicular to the axis of rotation. This means that the Y location of any point on the roller remains constant. If the point on the web contacts the roller without slipping, then that point should also remain in a plane having a constant Y location. This can be formulated as a multi-point constraint. It is required that all nodes on the roller have the same Y-displacement as the node having the same nominal Y coordinate that first contacts the roller. This is illustrated in figure 6.

When all of the constraints are combined, all of the degrees of freedom of the nodes on the roller are either fixed or are related to another node by a multi-point constraint.

THE SPREADING PROCESS

The next stage in modeling the spreading rollers is the actual spreading process. This process requires an iterative search for a set of cross machine direction displacements that are compatible with the condition of normal entry to the roller.

The search process can be posed as a nonlinear least squares curve fitting problem which in effect is a multidimensional nonlinear optimization problem. It can be stated as follows:

> Find the set of applied forces which minimize the sum of the squares of the deviations from normal entry to the roller. The minimum value of this sum in known in advance to be zero.

The set of applied forces can be selected in two ways. A force can be chosen independently for each node at the end of the entry span. This gives as many independent variables for the optimization process as there are nodes across the width of the web. For the mesh chosen, this would give an eleven dimensional optimization problem.

A better approach is to use a function to define the force distribution across these nodes. The problem then becomes one for finding the proper values for the coefficients of this function to minimize the least square error. This can greatly reduce the order of the optimization problem. The simplest choice for the forcing functions are simple polynomials.

The lowest order polynomial is a simple constant but this does not allow any variation of force across the roller width. It seems unlikely that this would allow all of the nodes to approach normal entry to the roller.

The next order polynomial is a straight line. The line is defined by two coefficients, and does allow a force variation. If the linear force profile allows sufficient variation in force to approach zero error, then the problem is reduced from an eleven variable optimization problem to a two variable problem. This turns the problem from one that would probably never converge to a reasonable solution into one that should converge in a relatively short time.

The linear force function was implemented in the spreading roller analysis program. This simple function allows the search to converge in a matter of minutes to very acceptable accuracy. The Nelder-Mead Simplex method was used to perform the optimization process. The objective function for the search is given in equation (1).

$$\sum_{i=1}^{N_w} \left((\text{Slope before roller}) - (\text{Slope after roller}) \right)^2 \qquad (1)$$

DEFORMATIONS AND STRESSES PREDICTED BY THE CONCAVE ROLLER MODEL

The distributions of deformations, stresses, and friction forces over the surface of the web are calculated for an example system by the spreading model program. The results are summarized using X-Y plots to display the spreading deformations, and 3-D contour lines to display the stress distributions.

Figure 7 shows the effective spreading produced by the model. The effective spreading is the relative cross-machine direction displacement with respect to the same point far upstream. It can also be viewed a the cross-machine direction deformation of a streamline. The first thing to notice is that the spread lines have zero slope beginning slightly before the point of contact with the roller, and ending at the last point of contact with the roller. This represents two of the essential properties of the concave roller model. First, the no slip boundary condition causes the displacements at the entrance of the roller to be transported over the roller. In addition, normal entry condition says that given sufficient friction, the web will spread so that streamlines approach the roller normal to the line of initial contact. For both of these, the normal direction is parallel to the machine direction, therefore the lines have zero slope.

The next thing to notice is that the spread lines converge to zero at the left and right sides of the plot. This does not mean that each of these streamlines have zero displacement at the ends or even the same displacement. Remember that each of these curves represents the deviation in displacement relative to the point at the beginning of the entry span. Each of the points at the beginning of the entry span have undergone a displacement because of the Poisson contraction. In this plot, the deviation of the curve from zero effective spreading represents the additional displacement beyond the Poisson contraction. At the left and right end, the only displacement in the web is the Poisson contraction. This means that the spreading effect is restricted to the area near the roller. For the parameter values chosen for the base case, the roller affects the web material about one web width upstream and downstream of the roller.

The final thing to note from these curves is the relative spreading. The curve at Y=0 has zero effective spreading everywhere. Because Y=0 is the symmetric centerline of the model, this is to be expected. It is also significant that the space between curves near the centerline is greater than the space between curves near the edge of the web. The total spreading force at any point along the width of the web is related to the distance of that point from the edge of the web. The total spreading force approaches zero as the point approaches the edge of the web.

Figure 8 shows the distribution of machine direction stresses. It shows that there is extreme variation in the MD stress. The variation is greatest near the roller, while the stresses approach a uniform value farther away from the roller. This uniform value is the nominal MD stress induced by the line tension.

The stresses are greatest near the edge of the roller, and smallest near the center of the roller. This was expected from simple geometric reasoning. The outer edges of the roller have a larger radius. The material must undergo larger strains and stresses to conform to this larger radius. In addition, the velocity at the outer edges is greater than the velocity at the center of the roller. This tends to shear the edges of the web ahead of the center, causing greater stresses near the edge. An interesting feature common to all of the stress plots for the concave roller is also shown in figure 8. The stress contours in the area where the web is in contact with the roller are all parallel to the machine direction. This is again a consequence of the no slip boundary condition which says that the state of strain immediately before the roller is transported over the surface of the roller.

Figure 9 shows the cross machine direction stress distribution for the concave roller model. The range of stresses in the cross machine direction is not as large as the range of machine direction stresses. The primary feature shown in the figure is the character of the CD stress distribution. The stresses are greatest near the center of the roller, decreasing to near zero at the edge of the roller. This stress distribution is consistent with the spreading displacement plot. The material at the edge of the roller has no spreading force applied to it. The material at the center of the roller is being pulled outward by the friction forces acting on the entire web, therefore incurring higher stresses.

It was surprising to see a large region of compressive CD stresses in the exit span. The magnitudes of those compressive stresses are small compared to the maximum CD tensile stress but are still significant. The existence of these compressive stresses can be explained as follows. The larger radius at the edge of the concave roller tends to shear the material at the edges of the web ahead of the material at the center. This shearing induces a MD stress profile with significantly larger tensile stresses near the edge of the web than at the center of the web. This stress profile acts as a force couple bending the edges of the web in toward the center at the exit span, causing compressive CD stresses in the exit span.

Figure 10 shows the shear stress distribution for the concave roller model. The shear stress distribution is consistent with the behavior expected from the roller geometry. The material at the edges of the roller is sheared ahead of the material at the center, therefore the shear stresses are higher at the edge. Because the web centerline is a line of symmetry, the shear stresses decrease to zero at the web centerline. The stress variation is greatest near the roller, decreasing to zero in the entry and exit span.

ANALYSIS OF PARAMETER VARIATIONS

The previous section examined the deformation and stress distribution over the entire web surface for a base set of parameter values. In this section, the parameters will be varied around those base values. This study required approximately 35 runs of the computer model. It is not feasible to discuss the resulting stress and deformation plots for each of those runs. Instead, representative values were tabulated from each of those runs, and combined in a set of summary plots. These summary plots were examined for trends in the response of the model to parameter variations.

These summary plots are organized in the following manner. For the range of values of a single parameter the following four plots are generated:

(1) Maximum effective spreading displacement (spreading beyond the Poisson contraction at the point on the outer edge of the web where it exits the roller)
(2) Maximum coefficient of friction required to enforce the predicted displacements
(3) Maximum and minimum machine direction (MD) stresses on a combined plot
(4) Maximum and minimum cross machine direction (CD) stresses on a combined plot

In each of these plots, the values in the list above are plotted on the vertical axis, and the values of the parameter being varied are on the horizontal axis.

The values for the parameters used in this study are given in

Table I. The values shown in bold print are the base parameter values for the roller. There were 36 plots generated in the analysis of parameter variations. Because of space limitations, only the plots for variation in the roller radius of curvature are given in this paper.

VARIATIONS IN ROLLER PROFILE RADIUS OF CURVATURE

It should not be surprising that the roller profile radius of curvature is the most significant parameter effecting the spreading behavior of the concave roller. Figures 11 through 14 show the effects of roller profile radius of curvature on the concave roller. The roller radius of curvature is intuitively the most significant parameter for the behavior of the roller. The roller curvature is the reason that the roller spreads the web. The amount of curvature is the only thing that differentiates this roller from simple cylindrical rollers. The curves show that the model produces results that match intuition.

The max spread and max friction curves show decreasing values with increasing radii of curvature. A radius of curvature of infinity produces a cylindrical roller. Thus, the behavior of the roller should approach the behavior of a cylindrical roller as the radius of curvature approaches infinity. For large radii, both the max spread and the max friction approach zero. In addition, both the max and the min MD stresses approach the nominal line tension, and the max and min CD stresses approach zero.

RESULTS

One of the limitations of the program arose from the need to produce and distribute models that do not require a mainframe or super-computer to give reasonable execution times. The current versions of the models do not allow slippage between the rollers and the web. Instead the models enforce the no-slip boundary condition, and report the resulting friction forces. For this reason, the current versions of the models are best used as tools to design rollers that do not slip. This is accomplished by varying roller geometry until the maximum friction requirements are lower than those known to be available.

The models can also be used to gain an understanding of existing spreading roller installations. By modeling the existing geometry, it can be determined whether or not the roller slips. This in itself is a significant piece of information. This model also gives an upper limit on the deformations and stresses in the web. If slipping occurs, both the deformations and stresses should be lower than those predicted.

Previous attempts at modeling these rollers allowed the web to conform to the doubly curved shape of these spreading rollers without incurring any strain in the material. Then the strains were simulated by adding local deformations. These local deformations had a significant effect on the calculated spreading. In the models produced by this research, the unstrained web was assembled around an average cylindrical roller. Then the correct set of boundary deformations was applied to cause the web to conform to the shape of the roller. This allowed both the web strains and deformations to be modeled more accurately.

In modeling the spreading process, nonlinear optimization techniques were used to find the correct set of spreading displacements. Those displacements were consistent with the fact that the streamlines in the web are steered to normal entry.

The most surprising conclusion reached from the concave roller model is the high values of coefficient of friction that are required to prevent slippage between the web and the roller. This is particularly true in the concave roller. The largest forces in the concave roller are the MD forces near the edges of the web. These are the forces that shear the edges of the web ahead of the center. Coefficients of friction greater than 1.0 were predicted for concave rollers having curvature values that were thought to be in a reasonable range.

RECOMMENDATIONS

The principal recommendations for extension of this work pertain to extending the capabilities in the model,. Three new capabilities in the model are of immediate interest to this author. First, the ability to allow slipping should be added. This will require a significant increase in computing power to perform the large number of iterations in a reasonable amount of time. Because of rapid improvements in computer speed, accompanied by reductions in price, machines capable of modeling slipping should be available to most engineers in the near future.

The model should also be modified to allow the web to move off of the centerline of the roller. Because these spreading rollers are de stabilizing devices, it would be useful to calculate the maximum displacement of the web centerline, and the resulting stress distribution. This would be a first step in modeling the lateral dynamics of webs on spreading rollers.

Finally, the spreading model should be combined with a wrinkle model to investigate the ability of these rollers to prevent wrinkling. A very simple wrinkle model might be a lateral compressive force or displacement distribution at some point in the entry span. The maximum compressive stress remaining at the entrance of the roller should be a good indication of the ability of the roller to prevent wrinkling.

ACKNOWLEDGMENTS

The authors of this paper would like to thank the sponsors of the Web Handling Research Center at Oklahoma State University for their finanicial and technical support of this research.

REFERENCES

1. "What is a Web" Unpublished Web Handling Research Center Information Brochure. Oklahoma State University, No date.
2. Swift, H. W., "Cambers for Belt Pulleys", Proceedings, Institute of Mechanical Engineers (London), Vol. 122, June, 1932, pp. 627-683.
3. Sassaki, Hira, Abe, Yangagishima, Shimoyama, and Tahara, "Control of Strip Buckling and Snaking in Continuous Annealing Furnace", Kawasaki Steel Technical Report, No. 9, March, 1984.
4. Shelton, J. J., "Fundamentals of Lateral Web Behavior", Unpublished Web Handling Research Center Information Brochure, Feb., 1988.
5. Shelton, J. J., and Reid, K. N., "Lateral Dynamics of an Idealized Moving Web", Journal of Dynamic Systems, Measurement, and Control, September, 1971, pp. 187-192.
6. Shelton, J. J., and Reid, K. N., "Lateral Dynamics of a Real Moving Web", Journal of Dynamic Systems, Measurement, and Control, September, 1971, pp. 180-186.
7. Shelton, J. J., "Dynamics of Web Tension Control with Velocity or Torque Control", Proceedings, 1986 American Control Conference, Seattle, Washington, Vol. 3, pp. 1423-1427.
8. Pfeiffer, J. D., "Web Guidance Concepts and Applications", TAPPI, Vol. 60, No. 12, December, 1977.
9. Butler, T., "How Concave Rolls Can Correct Dryer Fabric Bowing", Paper Trade Journal, Vol. 169, No. 3, March 1985, pp. 70-72.
10. Daly, D. A., "Factors Controlling Traction Between Webs and Their Carrying Rolls", TAPPI, Vol. 48, No. 9, Sept., 1965.
11. Leport, M. L., "The Mechanics of Webs Encountering Concave Rollers", M. S. Thesis, Oklahoma State University, 1987.
12. Kliewer, G. A., "Parametric Analysis of Webs Encountering Concave Rollers", M. S. Thesis, Oklahoma State University, 1988.
13. Zienkiewicz, O. C., The Finite Element Method in Structural and Continuum Mechanics, London, McGraw Hill, 1967.

TABLE I

Concave Roller Parameter Values

Thickness (in)	0.0005	0.0009	**0.0012**	0.0018
Machine Direction Modulus (psi)	50000	117000	**157000**	200000
Cross Direction Modulus (psi)	50000	**117000**	157000	200000
Machine Direction Poisson's Ratio	0.1	**0.16**	0.2	0.3
Web Width (in)	3	**6**	9	12
Line Tension (pli)	1.0	**1.5**	2.0	3.0
Roller Radius (in)	0.75	**1.125**	2.0	3.0
Roller Profile Radius of Curvature (in)	**1250**	2000	3000	5000
Wrap Angle (deg)	30	60	**90**	120

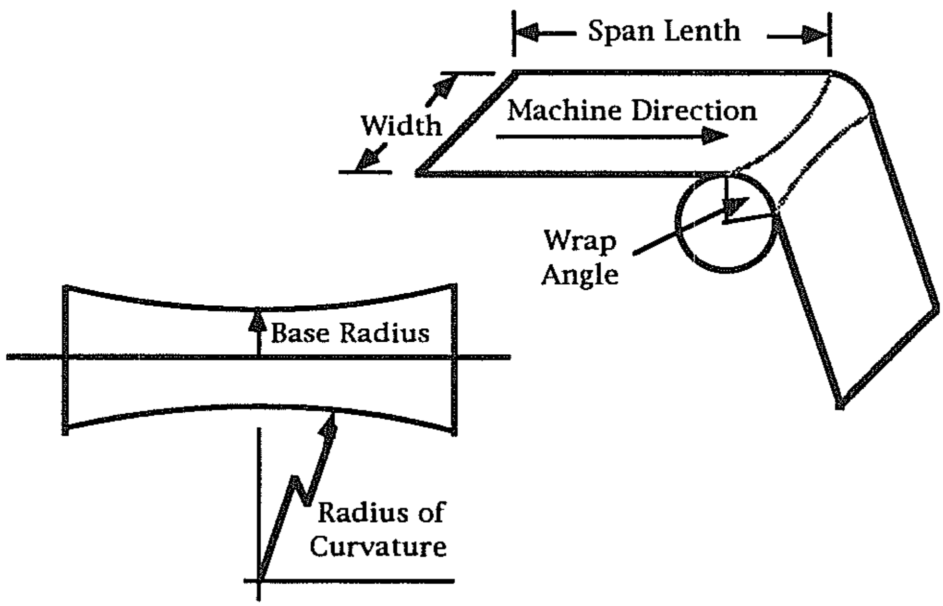

Figure 1. Concave Roller Nominal Dimensions

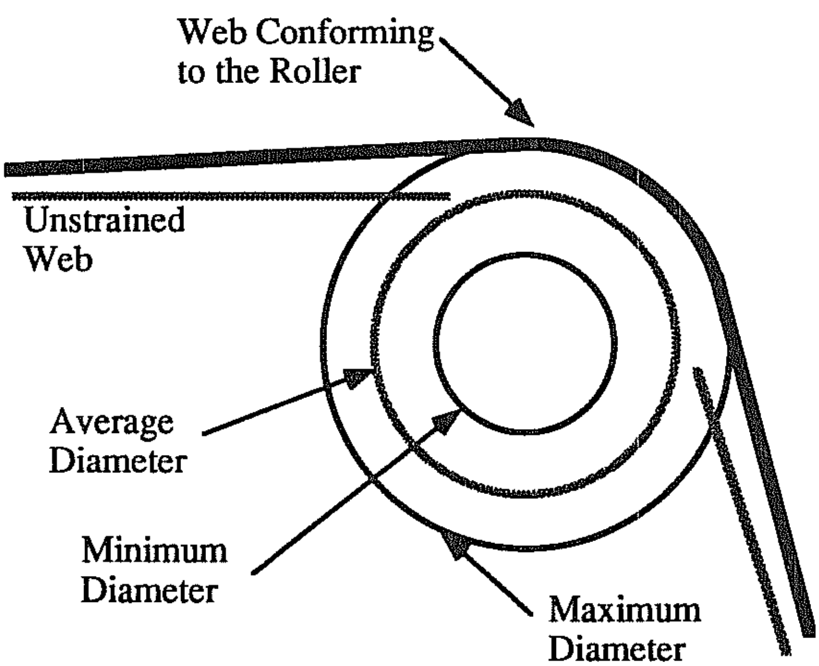

Figure 2. Web Deformed from Average Roller Diameter

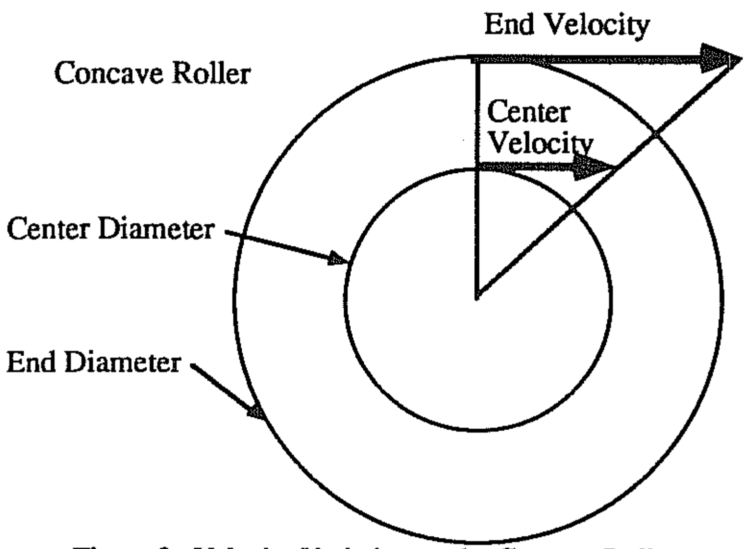

Figure 3. Velocity Variation on the Concave Roller

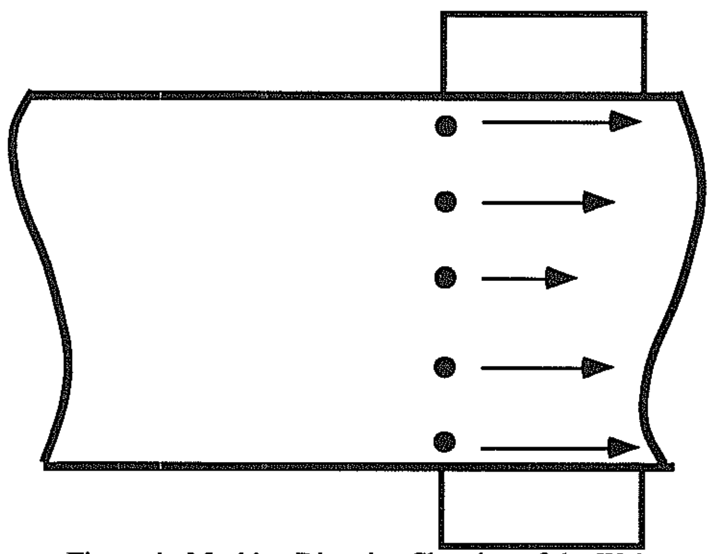

Figure 4. Machine Direction Shearing of the Web

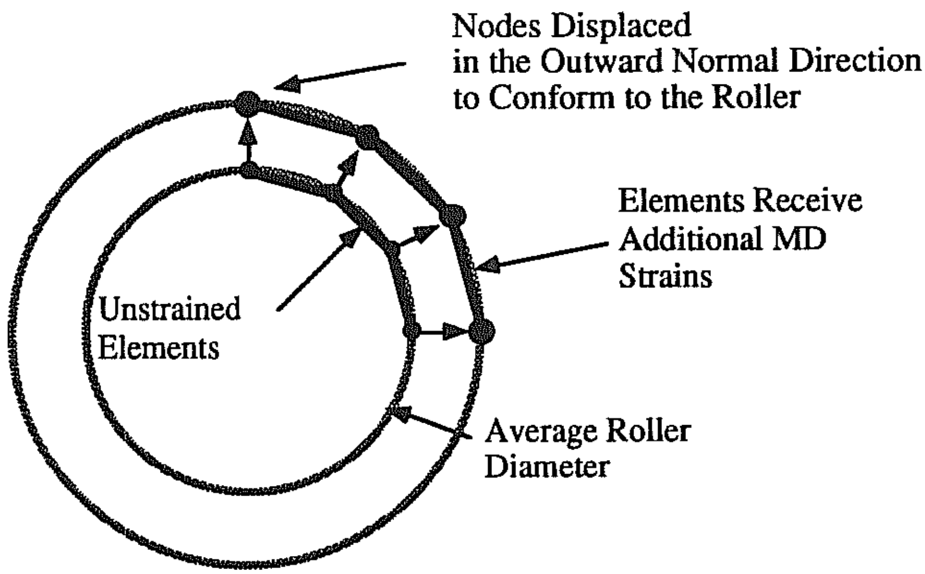

Figure 5. Machine Direction Strains Induced by Local Z-direction Displacements

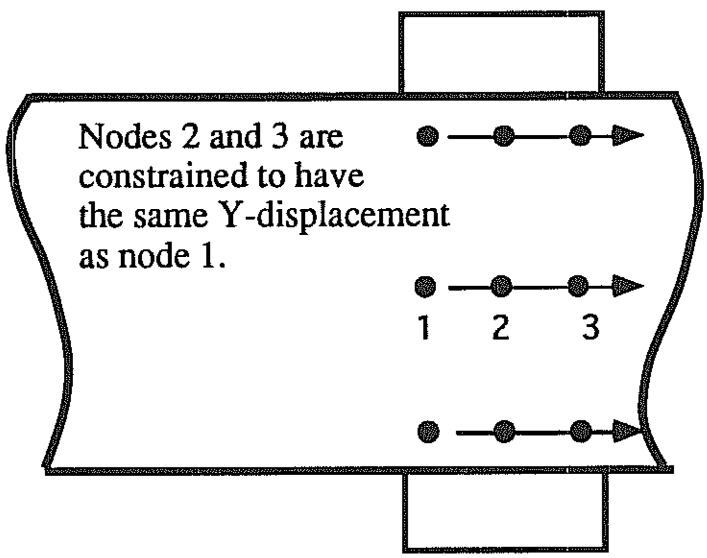

Figure 6. Y-lock Multi-point Constraints Over the Roller

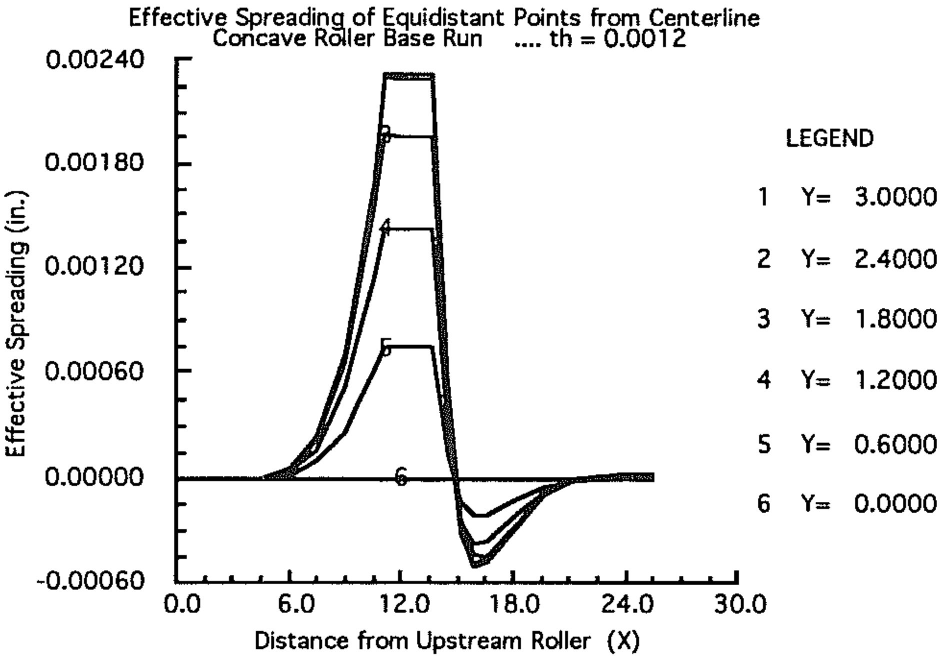

Figure 7. Concave Roller Base Run Effective Spreading

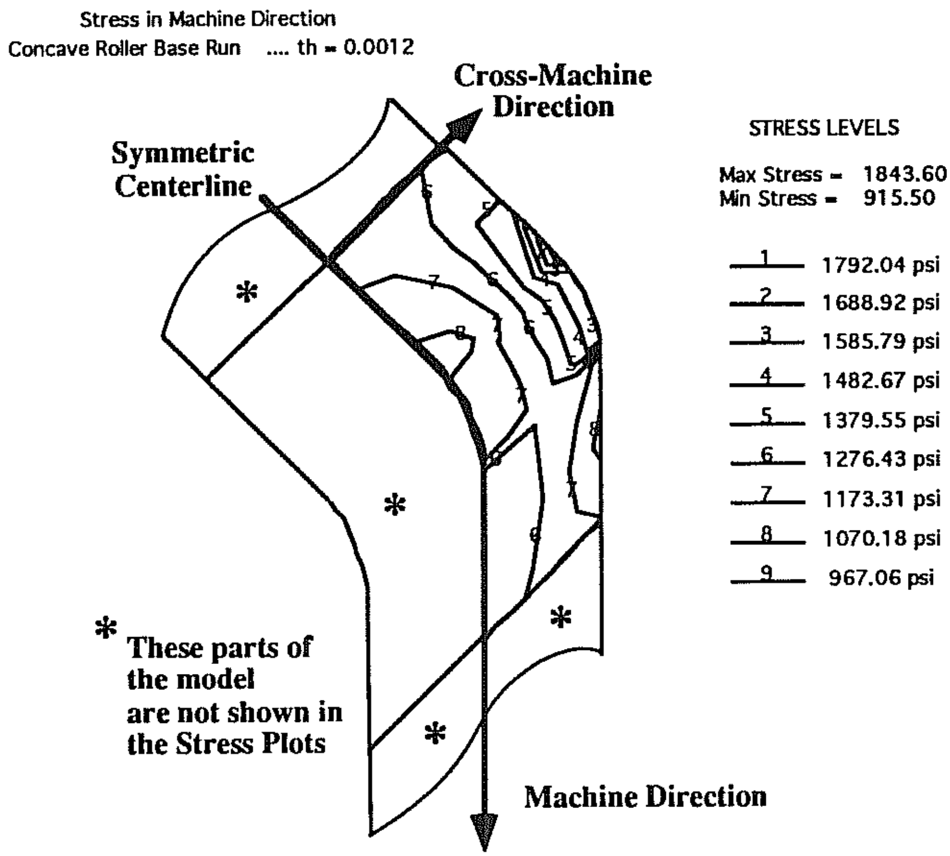

Figure 8. Annotated MD Stress Plot

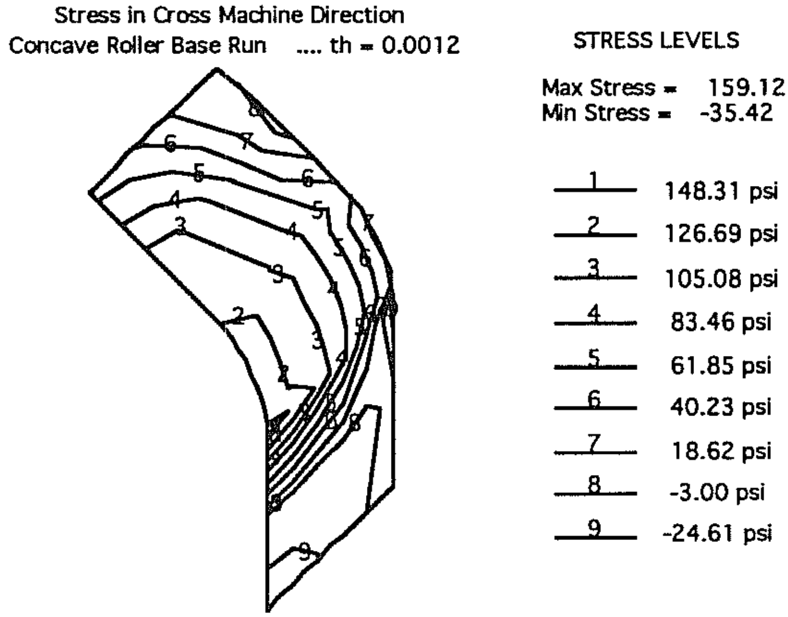

Figure 9. Concave Roller Base Run CD Stresses

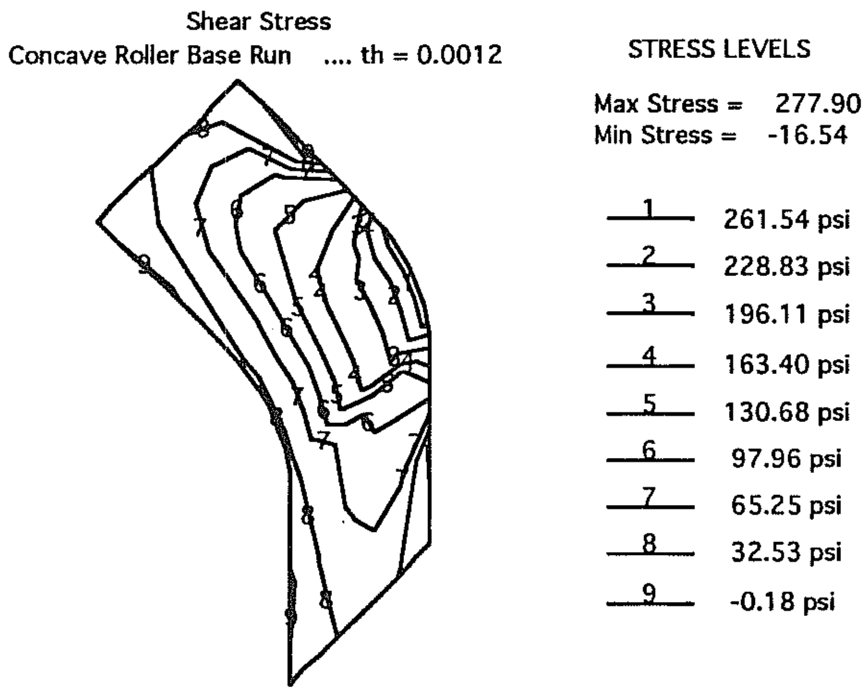

Figure 10. Concave Roller Base Run Shear Stresses

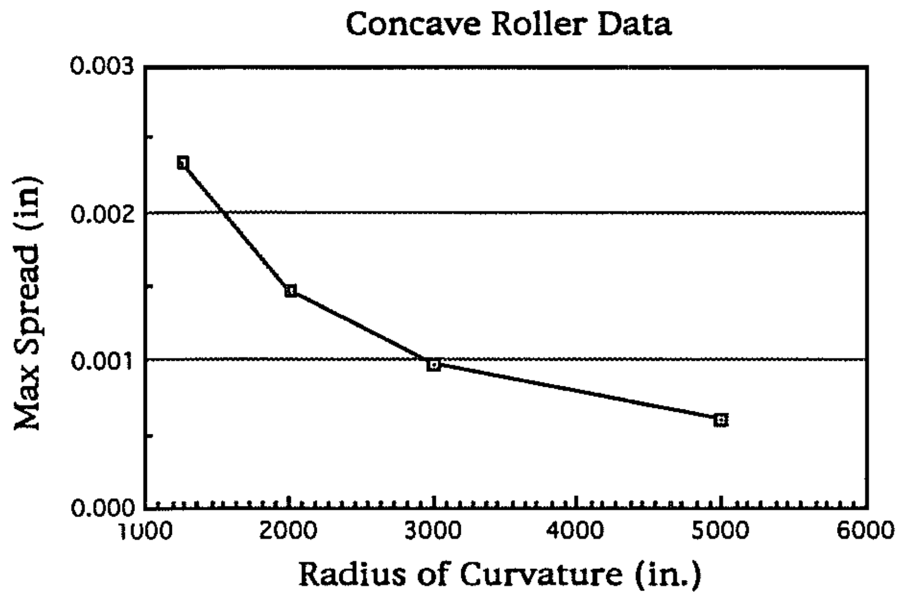

Figure 11. Concave Roller - Spread vs. Radius of Curvature

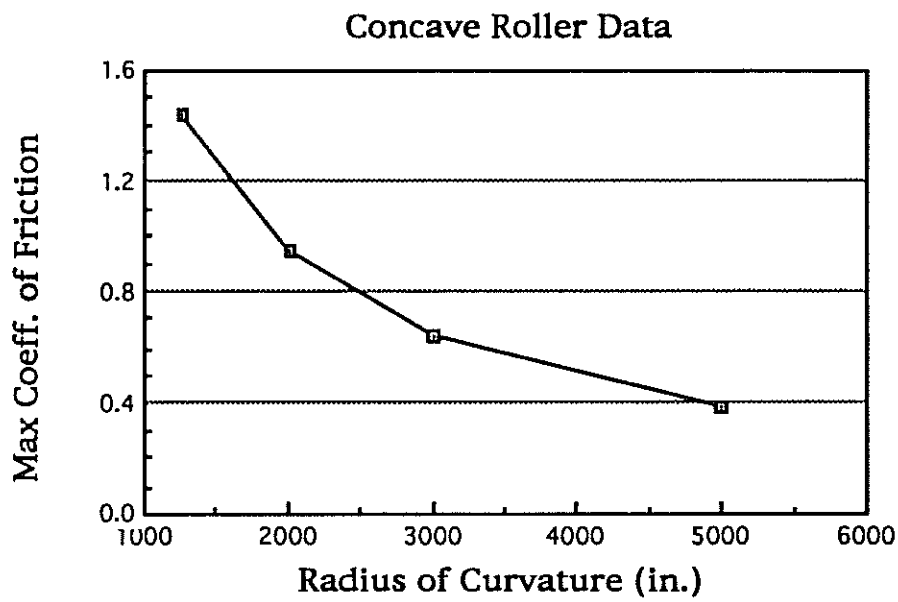

Figure 12. Concave Roller - Friction vs. Radius of Curvature

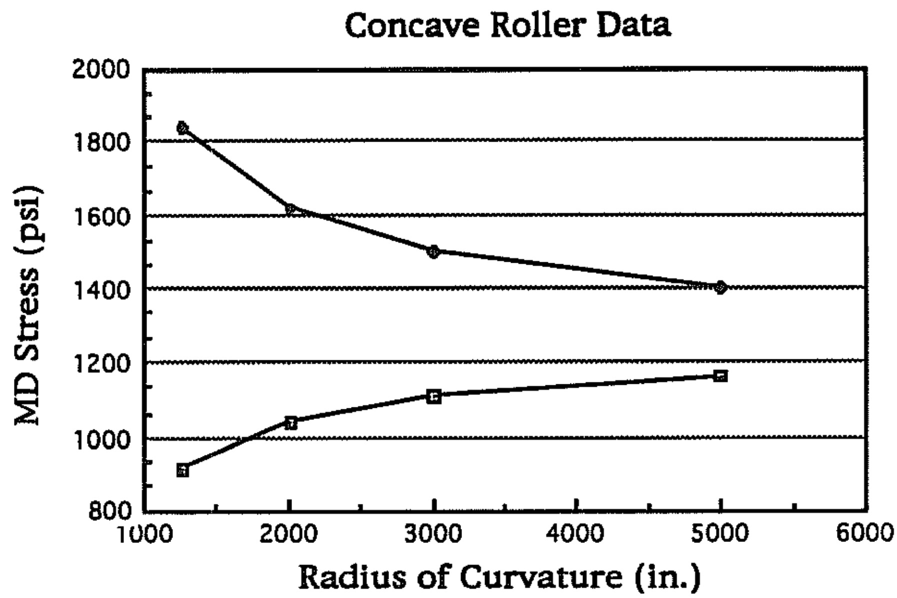

Figure 13. Concave Roller - MD Stress vs. Radius of Curvature

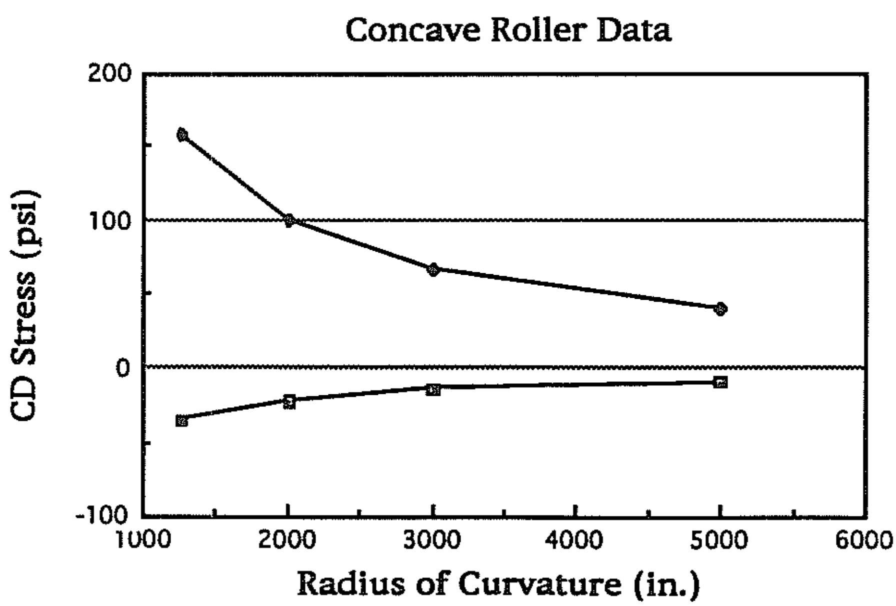

Figure 14. Concave Roller - CD Stress vs. Radius of Curvature

QUESTIONS AND ANSWERS

Q. What set of parameter values were used to generate the data for figure 7?

A. Well, that figure is for one set of parameters in the model, what I call my base set of parameters, and if you flip to Table 1, which shows the range of parameters that I studied, I think you'll notice that some of those numbers are in bold. All of the stress and displacement plots are for those numbers in bold. I call that my base set of parameters.

Q. Can extreme amounts of curvature in the roller actually cause greater wrinkling?

A. Yes, if you go to that kind of an extreme, that's correct. My understanding is that you should never be able to see with the naked eye, just glancing at a roller, you shouldn't be able to see the shape of the thing.

Q. Isn't it true that the spreading effect dissipates in about $1\frac{1}{2}$ inches?

A. That's absolutely correct. I'd have to look at the numbers. An inch and a half seems a little bit fast. This is a 6 inch wide web, and I would say that all of the effect is basically gone within a 1 web width from the roller.

Q. Have you considered modifying your model to incorporate slipping?

A. I already have, I'm simply not ready to report on it, but that model is working.